

# Animal Model

## Induction of Pathogenic Sets of Genes in Macrophages and Neurons in NeuroAIDS

Eleanor S. Roberts, Michelle A. Zandonatti, Debbie D. Watry, Lisa J. Madden, Steven J. Henriksen, Michael A. Taffe, and Howard S. Fox

*From the Department of Neuropharmacology, The Scripps Research Institute, La Jolla, California*

**The etiology of the central nervous system (CNS) alterations after human immunodeficiency virus (HIV) infection, such as dementia and encephalitis, remains unknown. We have used microarray analysis in a monkey model of neuroAIDS to identify 98 genes, many previously unrecognized in lentiviral CNS pathogenesis, whose expression is significantly up-regulated in the frontal lobe of simian immunodeficiency virus-infected brains. Further, through immunohistochemical illumination, distinct classes of genes were found whose protein products localized to infiltrating macrophages, endothelial cells and resident glia, such as CD163, Glut5, and ISG15. In addition we found proteins induced in cortical neurons (ie, cyclin D3, tissue transglutaminase,  $\alpha$ 1-antichymotrypsin, and STAT1), which have not previously been described as participating in simian immunodeficiency virus or HIV-related CNS pathology. This molecular phenotyping in the infected brains revealed pathways promoting entry of macrophages into the brain and their subsequent detrimental effects on neurons. These data support the hypothesis that in HIV-induced CNS disease products of activated macrophages and astrocytes lead to CNS dysfunction by directly damaging neurons, as well as by induction of altered gene and protein expression profiles in neurons themselves which are deleterious to their function. (*Am J Pathol* 2003, 162:2041–2057)**

The cognitive/motor disorder associated with human immunodeficiency virus (HIV), also known as the AIDS dementia complex or neuroAIDS, occurs in approximately one-third of patients infected with HIV. Symptoms range from a minor disorder affecting 25% of individuals to dementia affecting 15 to 20% of those with AIDS. In

symptomatic individuals, aspects of the pathological entity of HIV encephalitis (HIVE), which includes the appearance of infected cells of the monocyte/macrophage lineage, microglia/macrophage nodules, and multinucleated giant cells (MNGCs), have been proposed to correlate with neuroAIDS. Although many individuals with neuroAIDS do not exhibit frank HIVE, central nervous system (CNS) dysfunction best correlates with the level of activated microglia/macrophages in the brain as opposed to the level of viral infection.<sup>1</sup> Still, the etiology of HIV-induced CNS alterations remains unknown. Although cognitive dysfunction in HIV-infected individuals is linked to pathologically damaged neuronal dendrites,<sup>2</sup> the virus does not infect neurons thus indirect effects that follow infection of macrophage-like cells in the brain likely result in the neurological dysfunction of neuroAIDS.

Experimental infection with simian immunodeficiency virus (SIV) in rhesus macaques provides many parallels to HIV infection of humans including CNS infection and dysfunction. Cognitive and motor dysfunction, neurophysiological abnormalities, and neuropathological changes including SIV encephalitis (SIVE) are also found in SIV-infected monkeys.<sup>3</sup> As with the human disease, CNS abnormalities can occur throughout the course of infection, with the most severe symptoms at the onset of clinical AIDS. Like HIVE, SIVE can occur with end-stage disease and accompany CNS disorders.<sup>4</sup> SIVE arises sporadically in infected rhesus macaques, similar to HIVE in humans, but a reproducible system in which monkeys are transiently depleted of CD8+ cells shortly after infection<sup>5</sup> leads to rapid development of SIVE in a high percentage of animals.<sup>6</sup>

Macrophages and microglia can produce molecules that are potentially harmful to neurons. Although such products are common candidates in proposed pathogenic mechanisms mediating HIV/SIV-initiated damage to the CNS,<sup>7</sup> the identities of the molecules responsible

---

Supported by the National Institutes of Health (grants MH59468, MH61224, MH61692, MH62261, and RR13150).

This is manuscript no. 15012-NP from The Scripps Research Institute.

Accepted for publication February 17, 2003.

Address reprint requests to Howard S. Fox, Department of Neuropharmacology, CVN-1, The Scripps Research Institute, 10550 North Torrey Pines Rd., La Jolla, CA 92037. E-mail: hsfox@scripps.edu.

for neuropathogenesis remain unknown. We hypothesized that an unbiased examination of brain RNA from animals with SIV-induced CNS disease would allow us to identify gene transcripts found in infiltrating and activated macrophages, as well as other cell types in the affected brains, and to analyze their pathogenic products as well as molecular pathways of disease. To this end, gene expression was analyzed in the frontal lobe of brains from control and SIV-infected animals depleted of CD8+ cells during acute infection, using Affymetrix Human U95Av2 GeneChips to measure the expression of mRNA transcripts. We have found, as have others, that human gene chips are efficient in detecting mRNA transcripts from rhesus macaque tissues.<sup>8,9</sup> Indeed, here we report that many genes, previously unrecognized, were significantly up-regulated in the frontal lobe of brains with SIVE compared to that of uninfected animals. Using those results, we examined protein expression by immunohistochemistry to create a profile of the pathogenic cell populations present in the brain and to investigate the inflammatory processes and molecular alterations that result in CNS disease.

## Materials and Methods

### Rhesus Macaques

For this experiment we used 13 rhesus macaques free of SIV, type D simian retrovirus, and Herpes B virus, that were obtained from Charles River Breeding Laboratories (Key Lois, FL) and Covance (Alice, TX). Experiments were performed when the animals were 3 to 5 years of age with The Scripps Research Institute's Animal Care and Use Committee approval and guidelines. Seven macaques were intravenously inoculated with a cell-free stock of SIVmac182 (p27 *gag* antigen equivalent of 0.9 ng, diluted in RPMI 1640 for injection). After inoculation these animals were initially injected with 10 mg/kg (subcutaneous) then subsequently 5 mg/kg (intravenous) of the CD8 antibody cM-T807 at 6, 9, and 13 days after inoculation, a slight modification of the originally described protocol.<sup>5</sup> The SIVmac182-infected monkeys were sacrificed, after development of signs of simian AIDS, on the following days after inoculation: macaque no. 289 (72 days), no. 301 (108 days), no. 321 (108 days), no. 322 (214 days), no. 323 (93 days), no. 328 (79 days), and no. 330 (111 days).

All of the SIV-infected animals had abnormalities in CNS functional testing (neurophysiology, cognitive and motor tasks), which will be reported in detail (MA Taffe and colleagues, in preparation). On postmortem histopathological examination one monkey (no. 322) had a lymphoma involving the CNS and was subsequently excluded from the study. The remaining six monkeys all showed signs of SIV encephalitis (SIVE) with varying degrees of severity. This was defined as including microglia activation, macrophage infiltration, perivascular cuffing, macrophage/microglia nodules, and high CNS viral loads (>100,000 RNA equivalent copies of SIV per  $\mu$ g

frontal lobe RNA), with four of the cases also showing MNGCs (macaque nos.: 289, 301, 321, and 323).

The CD8+ cell-depleting regimen was also administered to two of six uninfected control monkeys (no. 392 and no. 393) who were sacrificed 87 and 113 days later, respectively. The four other uninfected control animals (no. 298, no. 331, no. 332, and no. 357) did not receive any treatment.

Necropsy was performed after terminal anesthesia (with ketamine, xylazine, and pentobarbital), with subsequent extensive intracardiac perfusion with sterile PBS containing 1 U/ml heparin to clear blood-borne cells from the brain tissue. A portion of the frontal lobe (from one sagittal section of the brain, cut coronally with the rostral border 0.5 cm from the frontal pole and the caudal border rostral to the head of the caudate) was taken for RNA extraction and preserved in RNA-Later (Ambion Inc., Austin, TX). Representative sections of this area were immersed in 10% formalin for histological studies. Additional brain tissue was taken from a coronal section of the occipital lobe in the striate area (control macaque nos.: 331, 392, 393; SIVE macaque nos.: 301, 321, 323, 330), midbrain (control macaque nos.: 298, 332, 357, 331; SIVE macaque nos.: 289, 301, 321, 323, 328), and a mid-sagittal section of cerebellum (control macaque nos.: 298, 332, 357, 331, 392, 393; SIVE macaque nos.: 289, 301, 321, 323, 328).

### DNA Array

Total RNA was purified from samples using TRIzol Reagent (Invitrogen, Carlsbad, CA) following the manufacturer's protocol, with an additional centrifugation step to remove unwanted cellular debris. RNA was then further purified using the RNeasy mini kit (Qiagen, Valencia, CA) and the quantity of total RNA was assessed by 260-nm UV absorption, with quality verified by gel electrophoresis and analysis of the ribosomal RNA bands. Total RNA was prepared to synthesize cDNA that was then used as a template to produce biotinylated cRNA (as described in the Gene Chip Expression Analysis Technical Manual, Version 5.0; Affymetrix, Santa Clara, CA). Affymetrix Test 2 chips were used to assess RNA quality by examining the 3' to 5' ratios for actin and glyceraldehyde-3-phosphate dehydrogenase (GAPDH). Fifteen  $\mu$ g of cRNA was prepared in a hybridization cocktail of 300  $\mu$ l total volume, of which 200  $\mu$ l was placed on an Affymetrix Human U95Av2 GeneChip, containing 12,625 independent probe sets to analyze gene expression. After hybridization this sample was returned to the original aliquot, which was then frozen. For the frontal lobe samples, a further 200  $\mu$ l was sampled from the original cocktail and hybridized to a separate duplicate GeneChip within 30 days. Hybridization and subsequent washing and staining were performed using the Affymetrix Fluidics Station 400 following supplied protocols. Chips were then double stained and scanned according to basic Affymetrix protocol to create GeneChip image files that were converted to text-bases files using Microarray Suite 5.0 software (Affymetrix).

**Table 1.** Antibody Dilutions Used for Immunohistochemistry

Antigen	Dilution	Antigen recovery	Antibody type	Source
Alpha-1 antichymotrypsin	1:200	None	Rabbit poly	Novacastra
Apolipoprotein D	1:100	Citrate	Mouse mono	Novacastra
C1q	1:4	None	Rabbit poly	BioGenex
CD163	1:100	Citrate	Mouse mono	Novacastra
CD31	1:50	Citrate	Mouse mono	Dako
CD37	1:300	Citrate	Mouse mono	Novacastra
Cyclin D3	1:40	Citrate	Mouse mono	Novacastra
GFAP	1:500	Citrate	Rabbit poly	Zymed
Glut5	1:200	Citrate	Rabbit poly	Chemicon
HAM56	1:200	Citrate	Mouse mono	Dako
HLA-DR (LN3)	1:50	Citrate	Mouse mono	Zymed
ISG15	1:250	Citrate	Rabbit poly	Dr. E. Borden
LCA	1:300	Citrate	Mouse monos	Dako
STAT1	1:100	Citrate	Mouse mono	Santa Cruz
TGase II (Ab-3)	1:250	Citrate	Mouse monos	Neomarkers
Vimentin	1:100	Citrate	Mouse mono	Novacastra
Von Willebrand Factor	1:300	None	Rabbit poly	Dako

Earlier versions of the Affymetrix software gave empirical Average Difference values that could be negative and thus compromise statistical analysis. In this newer version each oligomer was assessed for signal intensity, and a mean Signal Value (SV) was obtained that assigns to the transcript a relative measure of abundance that is always a positive number. GeneSpring Expression Analysis Software 4.1 (Silicon Genetics, Redwood City, CA) was then used for statistical analysis of the SVs for each gene between the groups. Individual cases were classified for comparison as either control or SIVE. Cases were analyzed after normalization to center the data around 1. Next, significant differences in expression levels for the frontal lobe samples were determined to highlight only up-regulated genes as follows: 1) mean normalized SV of the SIVE group of at least 0.8 (to select for a significant level of expression of up-regulated genes, equivalent to a prenormalization SV of 200), 2) fold-change in mean normalized SV between SIVE and control of at least two-times higher, and 3)  $P < 0.01$  using a nonparametric test (Wilcoxon-Mann-Whitney). As stated, these criteria highlight only significantly up-regulated genes. Discussion of down-regulated genes will be presented in a subsequent article. For the comparison of other brain regions, a single GeneChip analysis was performed from each sample, and the control and SIVE samples were grouped separately from each region and analyzed, using criteria 1 and 2 above, for the presence of probe sets that had been found to be up-regulated in the frontal lobe.

### *Immunohistochemistry and in Situ Hybridization*

After identification of significantly up-regulated genes, this analysis was used for an immunohistochemical/*in situ* hybridization study of the location of proteins or transcripts corresponding to 16 of the up-regulated genes. In addition to the tissue from animals used in the array analysis, two more SIV-infected animals, that did not receive the CD8+ cell-depleting antibody but developed SIVE spontaneously in the course of simian AIDS, were used in the immunohistochemical studies for comparison

with the SIV-infected monkeys given the CD8+ cell depleting regime. These animals were no. 188 (sacrificed at 308 days after inoculation) and no. 226 (sacrificed at 378 days after inoculation).

Formalin-fixed, paraffin-embedded sections were deparaffinized with xylene and hydrated in graded alcohols. Immunohistochemical staining followed a basic indirect protocol, using an antigen retrieval method where indicated (heating to 95°C in 0.01 mol/L citrate buffer for 45 minutes, then left for 20 minutes to steep). Antibodies and protocols used are indicated in Table 1. The primary antibody was detected with the PicturePlus universal secondary antibody-horseradish peroxidase polymer reagent (Zymed, San Francisco, CA) and developed with the NovaRed chromogen (Vector Laboratories, Burlingame, CA), followed by a hematoxylin counterstain (Sigma-Aldrich, St. Louis, MO). Control slides included omission of the primary antibody and use of irrelevant primary antibodies.

*In situ* hybridization was performed using probes for rhesus ISG12 and HCgp39, which were obtained by reverse transcriptase-polymerase chain reaction amplification using oligonucleotides derived from the human sequence. Molecularly cloned products were verified by DNA sequencing and used to construct <sup>33</sup>P-labeled RNA probes (Stratagene, Cedar Creek, TX) with RNA bacteriophage promoters. Formalin-fixed, paraffin-embedded sections were prepared for immunohistochemistry as above, with heat-treatment in citrate buffer; after washes in 0.5× standard saline citrate, sections were incubated for 1 hour at 42 to 46°C in a prehybridization buffer (50% formamide, 0.3 mol/L NaCl, 20 mmol/L Tris, pH 8, 5 mmol/L ethylenediaminetetraacetic acid, 1× Denhardt's solution, 10 mmol/L dithiothreitol, 10% dextran sulfate in diethyl pyrocarbonate-treated water) and subsequently hybridized in 3 × 10<sup>6</sup> cpm radiolabeled probe in the same buffer at 42 to 46°C overnight. Controls included sense probes and omission of the probe. After hybridization, sections were washed and treated with RNase fol-

**Table 2.** Genes Up-Regulated in the Frontal Lobe of SIVE Cases Compared to Control Cases

Control	SIVE	Fold change	Probe set	Accession number	Gene name	OL	MB	CB
<b>Monocyte migration</b>								
0.50 (0.27)	1.07 (0.33)	2.1	37398_at	AA100961	CD31/PECAM	*		
2.01 (1.36)	5.21 (1.56)	2.6	41138_at	M16279	CD99/MIC2			
0.87 (0.22)	1.94 (0.56)	2.2	31719_at	X02761	Fibronectin	*		*
0.50 (0.22)	1.45 (1.02)	2.9	31720_s_at	M10905	Fibronectin	*		
0.35 (0.37)	1.40 (0.61)	3.9	311_s_at	HG3044-HT3742	Fibronectin	*		
0.39 (0.19)	0.89 (0.52)	2.3	32526_at	AA149644	JAM3			
2.30 (0.71)	7.78 (4.34)	3.4	2092_s_at	J04765	Osteopontin	*		
15.47 (4.30)	40.95 (18.04)	2.7	34342_s_at	AF052124	Osteopontin	*		
0.25 (0.12)	0.82 (0.64)	3.2	38138_at	D38583	S100A11/Calgizzarin			*
0.51 (0.42)	1.97 (0.66)	3.8	38404_at	M55153	Transglutaminase-2	*	*	*
<b>Inflammation and disease</b>								
0.31 (0.19)	1.23 (0.49)	4.0	36781_at	X01683	Alpha1-antitrypsin	*	*	
0.55 (0.36)	1.43 (0.45)	2.6	33825_at	X68733	Alpha 1-antichymotrypsin	*	*	
6.03 (1.83)	14.39 (3.66)	2.4	32242_at	AL038340	Alpha B-crystallin	*		
17.25 (6.45)	36.63 (8.66)	2.1	32243_g_at	AL038340	Alpha B-crystallin			
0.46 (0.40)	1.79 (1.37)	3.9	36681_at	J02611	Apolipoprotein D	*	*	
0.57 (0.40)	1.24 (0.67)	2.2	39775_at	X54486	C1-inhibitor			*
0.41 (0.28)	3.66 (0.91)	9.0	38796_at	X03084	C1q-B	*	*	
0.72 (0.37)	3.88 (1.32)	5.4	40766_at	U24578	C4a	*	*	
0.58 (0.34)	1.42 (0.31)	2.5	34362_at	M55531	Glut5	*	*	
0.26 (0.24)	1.24 (0.51)	4.7	36197_at	Y08374	HCgp39/YKL-40	*	*	
0.97 (0.32)	2.59 (2.44)	2.7	33273_f_at	X57809	Heat shock 70kD protein 1A			*
0.43 (0.28)	1.43 (0.69)	3.4	36804_at	M34455	Indoleamine 2,3-dioxygenase	*	*	*
0.32 (0.27)	2.69 (0.99)	8.3	37754_at	L13210	Mac-2 binding protein	*	*	*
0.45 (0.36)	0.96 (0.5)	2.1	35426_at	AC004410	SPPL2b/PSL1			
0.17 (0.05)	1.88 (2.03)	11.0	1693_s_at	D11139	TIMP1			*
0.63 (0.29)	1.27 (0.20)	2.0	33452_at	M15518	Tissue plasminogen activator	*		
0.21 (0.17)	0.87 (0.31)	4.2	607_s_at	M10321	von Willebrand factor			*
<b>Antigen presentation</b>								
0.65 (0.36)	2.51 (0.98)	3.9	34644_at	AB021288	Beta 2-microglobulin	*	*	*
1.18 (0.57)	6.59 (3.19)	5.6	201_s_at	S82297	Beta 2-microglobulin	*	*	*
2.33 (1.06)	9.71 (3.59)	4.2	428_s_at	V00567	Beta 2-microglobulin	*	*	*
0.70 (0.60)	1.64 (0.32)	2.4	38363_at	W60864	DAP12			
1.21 (0.33)	3.32 (0.80)	2.7	41237_at	D32129	HLA-A	*	*	
2.02 (0.75)	15.16 (4.51)	7.5	37383_f_at	X58536	HLA-C	*	*	
0.38 (0.19)	1.59 (0.54)	4.2	37344_at	X62744	HLA-DM $\alpha$	*	*	
0.48 (0.24)	2.14 (1.41)	4.4	41723_s_at	M32578	HLA-DR $\beta$ 1	*	*	
1.82 (0.33)	8.15 (4.40)	4.5	32321_at	X56841	HLA-E	*	*	
1.76 (0.46)	6.28 (1.61)	3.6	37421_f_at	AL022723	HLA-F	*	*	
2.44 (0.68)	8.28 (2.54)	3.4	40369_f_at	AL022723	HLA-F	*	*	
0.98 (0.38)	5.57 (1.25)	5.7	40370_f_at	M90683	HLA-G	*	*	
0.87 (0.34)	4.01 (1.55)	4.6	35016_at	M13560	Ia-associated invariant $\gamma$ -chain/CD74	*	*	
1.13 (0.22)	2.96 (0.70)	2.6	36600_at	L07633	PA28 $\alpha$	*	*	
1.65 (0.44)	4.47 (1.08)	2.7	41171_at	D45248	PA28 $\beta$	*	*	*
1.82 (0.40)	4.06 (1.38)	2.2	1184_at	D45248	PA28 $\beta$	*	*	
0.07 (0.02)	0.86 (0.65)	12.0	41184_s_at	X87344	PSMB8/LMP7			*
0.99 (0.36)	5.06 (2.36)	5.1	38287_at	AA808961	PSMB9/LMP2	*	*	*
<b>Lysosomal</b>								
0.86 (0.65)	2.16 (1.23)	2.5	39062_at	AL008726	Cathepsin A			*
0.73 (0.30)	1.55 (0.56)	2.1	37021_at	X16832	Cathepsin H			*
0.56 (0.40)	1.20 (0.20)	2.2	32824_at	AF039704	CLN2	*		
0.46 (0.33)	1.67 (0.91)	3.6	39728_at	J03909	GILT/IP30	*	*	*
0.26 (0.16)	1.20 (0.73)	4.6	925_at	J03909	GILT/IP30	*	*	
1.08 (0.36)	3.18 (0.68)	2.9	37759_at	U51240	LAPTM-5	*	*	
0.62 (0.46)	1.38 (0.31)	2.2	39130_at	AB018313	Vam6/Vps39-like			
<b>Interferon inducible</b>								
0.20 (0.16)	1.64 (0.98)	8.4	1358_s_at	U22970	G1P3	*	*	
0.56 (0.21)	4.40 (1.52)	7.8	37641_at	D28915	IFI44	*	*	*
0.94 (0.15)	5.58 (2.43)	5.9	32814_at	M24594	IFIT1	*	*	*
1.47 (0.43)	18.33 (10.55)	12.0	915_at	M24594	IFIT1	*	*	*
0.41 (0.24)	2.87 (2.26)	7.0	908_at	M14660	IFIT2	*	*	
0.28 (0.20)	1.22 (0.58)	4.4	909_g_at	M14660	IFIT2	*	*	
0.29 (0.15)	0.94 (0.18)	3.3	38584_at	AF026939	IFIT4	*	*	*
0.38 (0.19)	0.84 (0.55)	2.2	675_at	J04164	IFITM1	*	*	*
5.51 (2.28)	61.23 (18.97)	11.0	676_g_at	J04164	IFITM1			*
3.66 (2.34)	35.11 (18.30)	9.6	41745_at	X57352	IFITM3	*	*	
0.38 (0.30)	5.79 (2.54)	15.0	425_at	X67325	ISG12	*	*	*
1.05 (0.35)	10.01 (7.22)	9.6	1107_s_at	M13755	ISG15	*	*	*
0.25 (0.19)	0.92 (0.97)	3.7	38432_at	AA203213	ISG15		*	*

(Table continues)

**Table 2.** *Continued*

Control	SIVE	Fold change	Probe set	Accession number	Gene name	OL	MB	CB
<b>Antiviral</b>								
3.75 (1.63)	9.54 (2.49)	2.6	38014_at	X79448	Adenosine deaminase	*	*	
0.13 (0.09)	3.00 (2.07)	23.0	37014_at	M33882	MxA/p78	*	*	
0.36 (0.21)	0.83 (0.51)	2.3	39264_at	M87284	2'-5'-oligoadenylate synthetase			
<b>Transcriptional regulation</b>								
2.48 (0.85)	6.24 (1.77)	2.5	38354_at	X52560	NF-IL6			*
1.20 (0.28)	2.54 (0.92)	2.1	1052_s_at	M83667	NF-IL6b	*	*	
0.52 (0.40)	1.23 (0.75)	2.4	38517_at	M87503	P48 protein/ISGF3 $\gamma$	*	*	
0.57 (0.14)	1.95 (1.00)	3.4	36423_at	W47047	P8 protein	*	*	
0.52 (0.40)	1.11 (0.35)	2.1	34189_at	D31891	SETDB1			
0.34 (0.13)	2.33 (0.68)	6.9	32859_at	M97935	STAT1 91kDa	*	*	*
0.35 (0.18)	1.13 (0.29)	3.2	32860g_at	M97935	STAT1 91kDa	*	*	*
0.17 (0.09)	3.11 (1.30)	18.0	3338_at	M97936	STAT1 91kDa	*	*	*
0.63 (0.29)	2.96 (1.32)	4.7	33339_g_at	M97936	STAT1 91kDa	*	*	
0.91 (0.42)	2.01 (0.75)	2.2	39708_at	L29277	STAT3	*		
0.95 (0.65)	2.03 (0.65)	2.1	39681_at	AF060568	Zinc finger protein 145 (PML)			
<b>Cell cycle</b>								
0.82 (0.57)	2.39 (0.97)	2.9	36131_at	AJ012008	CLIC1/NCC27	*	*	
0.60 (0.44)	1.26 (0.49)	2.1	1794_at	M92287	Cyclin D3			
0.82 (0.83)	2.96 (1.61)	3.6	32609_at	AI885852	Histone H2A	*	*	
0.51 (0.30)	1.13 (0.43)	2.2	35576_f_at	AL009179	Histone H2B	*		
0.34 (0.30)	0.83 (0.40)	2.4	34027_f_at	AA010078	Histone H4	*	*	
0.61 (0.59)	1.43 (0.40)	2.3	1787_at	U23398	p57KIP2	*		
1.56 (0.83)	3.33 (0.94)	2.1	39286_at	D64109	TOB2	*		
<b>Growth, differentiation, and signaling</b>								
0.55 (0.28)	1.42 (0.69)	2.6	1278_at	HG162-HT3165	AXL	*		
0.23 (0.12)	1.32 (0.97)	5.7	39061_at	D28137	BST-2	*	*	
3.95 (1.82)	9.43 (1.96)	2.4	35282_r_at	M33680	CD81/TAPA-1			
0.27 (0.07)	1.03 (0.67)	3.8	41198_at	AF055008	Epithelin/Granulin			*
2.73 (2.58)	6.81 (2.55)	2.5	424_s_at	X66945	FGFR1			
0.53 (0.35)	1.32 (0.43)	2.5	34268_at	X91809	GAIP/RGS19			
0.40 (0.25)	0.91 (0.62)	2.3	577_at	M94250	Midkine			*
2.03 (0.54)	4.39 (1.94)	2.2	31508_at	S73591	VDUP1/TBP-2			*
<b>Cytoskeleton</b>								
0.68 (0.21)	1.44 (0.51)	2.1	406_at	X53587	Integrin beta 4			
0.66 (0.35)	1.83 (0.63)	2.8	38391_at	M94345	Macrophage capping protein/CapG			*
1.72 (0.79)	4.03 (1.46)	2.4	40771_at	Z98946	Moesin			
3.54 (1.68)	7.32 (1.67)	2.1	38021_at	U53204	Plectin			
1.29 (0.63)	2.73 (0.66)	2.1	36902_at	X61587	RhoG			
9.27 (2.62)	19.47 (6.77)	2.1	34091_s_at	Z19554	Vimentin	*		
<b>Immune system</b>								
0.31 (0.06)	1.65 (0.70)	5.3	36661_s_at	X06882	CD14	*	*	
0.96 (0.36)	3.85 (1.03)	4.0	31870_at	X14046	CD37			
0.37 (0.18)	1.15 (0.87)	3.1	31438_s_at	Z22971	CD163/M130	*	*	
0.42 (0.41)	1.16 (0.39)	2.8	36889_at	M33195	Fc- $\epsilon$ receptor $\gamma$ -chain			
0.09 (0.05)	1.26 (1.90)	14.0	38194_s_at	M63438	Immunoglobulin kappa	*	*	
0.33 (0.21)	1.60 (2.22)	4.9	33274_f_at	M18645	Immunoglobulin lambda			*
0.34 (0.28)	0.89 (0.19)	2.6	34660_at	AI142565	Ribonuclease K6	*	*	
<b>Other</b>								
1.35 (0.85)	2.76 (0.72)	2.0	33804_at	U43522	Cell adhesion kinase beta			
1.21 (0.74)	2.58 (0.62)	2.1	41168_at	AF029750	CNPase			
0.35 (0.25)	1.08 (0.28)	3.1	38788_at	M82827	Fusion protein	*	*	
1.06 (0.51)	2.19 (0.48)	2.1	40054_at	D43949	KIAA0082			
0.23 (0.31)	1.15 (0.45)	4.9	32317_s_at	U34804	STP2			*
0.69 (0.53)	1.63 (0.34)	2.3	39693_at	N53547	Unknown			
0.20 (0.13)	0.94 (1.06)	4.8	41827_f_at	AI932613	Unknown			*

Average normalized SV, and (SD) for each probe set is indicated for the control and SIVE groups, followed by the fold change (SIVE/control). The GenBank ([www.ncbi.nlm.nih.gov](http://www.ncbi.nlm.nih.gov)) or Institute for Genomic Research ([www.tigr.org](http://www.tigr.org)) accession number from which each probe set was derived, the name of the Affymetrix probe set (sequences of the probes sets and links to gene information can be obtained at [www.affymetrix.com](http://www.affymetrix.com)), and the name of the gene represented by the probe set, are indicated.

\*indicates up-regulation of the gene probe sets in occipital lobe (OL), midbrain (MB), and cerebellum (CB).

lowed by an immunohistochemical staining with HAM56 antibody, performed as above except HistoMark Orange (KPL, Gaithersburg, MD) was used as the chromogen. The slides were then washed, dehydrated, vacuum-dried, and coated with LM1 emulsion (Amersham, Piscataway, NJ). The slides were then left in the dark for 40 days before developing (Kodak D19) and fixing (Kodak

'Fixer') (Eastman Kodak, Rochester, NY) followed by counterstaining with hematoxylin (Sigma-Aldrich), dehydrating, and mounting.

Image capture was performed with a Spot RT Color CCD camera with Spot RT software, version 3.4.2 for MacOS (Spot Diagnostic Instruments, Sterling Heights, MI) using a Leica Diaplan microscope (Leica Inc., Deerfield, IL). Fig-

ures were assembled with Adobe Photoshop, version 6.0 for MacOS (Adobe Systems Inc., San Jose, CA).

## Results

### *Array Analysis of SIV-Induced CNS Transcripts*

Statistical analysis revealed that 114 probe sets were significantly elevated in the frontal lobe of six monkeys with SIVE compared to six uninfected controls. These 114 probe sets corresponded to 98 independent genes (two or more probe sets were up-regulated for 12 genes). The mean SVs (plus SD) and fold change after normalization, accession numbers, probe sets, and gene names are listed in Table 2. As SIVE neuropathology was varied among the cases analysis was also performed to compare controls with only the SIVE cases that showed MNGCs; there were no significant differences between these cases and the comparison including those without MNGCs. Initially, the genes have been categorized based on the described biological properties of their products, but we note that many gene products can function in more than one category. The roles of several genes in these categories are detailed below.

### *Monocyte Migration*

HIV and SIV likely make their entrance into the CNS carried by infiltrating macrophages. Because these cells are of prime importance in the pathogenic effects leading to CNS dysfunction, the up-regulated genes involved with cell migration across the blood-brain barrier are grouped together here.

The migration of monocytes across endothelial junctions involves the sequential expression of CD31/platelet-endothelial cell adhesion molecule (PECAM) and CD99/MIC2.<sup>10</sup> Also involved is the macrophage scavenger receptor CD163, which is important in monocyte adherence to the vascular endothelium.<sup>11</sup> Tissue transglutaminase (tTG), an enzyme involved in the cross-linking of glutamine and lysine, serves as an adhesion and migration receptor for the extracellular matrix protein fibronectin, promoting the invasion of monocytes into tissues.<sup>12</sup> Osteopontin, a protein also involved in immune cell differentiation and activation, is a potent chemoattractant for monocytes,<sup>13</sup> thus increases in this molecule may also promote monocyte entry.

### *Inflammation and Disease*

The genes in this category are involved in inflammatory and neurodegenerative disorders of the CNS including HIV/SIVE. Indoleamine 2,3-dioxygenase (IDO) is an interferon (IFN)-inducible enzyme in the conversion pathway of tryptophan to the neurotoxin quinolinic acid, present in the brains of HIV-infected humans and SIV-infected monkeys.<sup>14</sup> The serine protease tissue-type plasminogen activator (tPA) is a crucial component of excitotoxin-induced microglial activation and neuronal

degeneration in the brain.<sup>15</sup> Increases in tPA in conjunction with matrix metalloproteinases can lead to degradation of the extracellular matrix unless the latter is blocked by the tissue inhibitors of metalloproteinases (TIMPs) such as TIMP1. SPPL2b/PSL1 (presenilin-like protein 1) is an intramembrane protease similar to the presenilins, thought to be crucial in Alzheimer's disease pathogenesis.<sup>16</sup> Levels of apolipoprotein D (ApoD), a transporter of cholesterol and arachidonic acid, are increased in the brains of those with stroke, Alzheimer's disease, and motor neuron disease.<sup>17,18</sup> Up-regulation of von Willebrand factor (vWf) indicates persistent activation of endothelial cells after injury. This factor is also released into plasma and elevated in correspondence with HIV progression and viral load.<sup>19</sup> Also in this category are GLUT5 and HCgp39, which are expressed in activated microglia and macrophages, respectively.

Three inflammation-related serine proteinase inhibitors were found to be up-regulated: C1 inhibitor (C1I);  $\alpha$ 1-antitrypsin and  $\alpha$ 1-anti-chymotrypsin (ACT). The latter two are major components of amyloid plaques in brains afflicted with Alzheimer's disease<sup>20</sup> along with complement component C1q.<sup>21</sup> Both C1I and ACT are tTG substrates (see *Monocyte Migration*), a link that connects the expression of these inflammatory components to the cell migration process.

### *Antigen Presentation*

Among the largest categories of genes described here are those involved in antigen presentation including both the major histocompatibility complex (MHC) class I and class II pathways for endogenous and exogenous peptide presentation to CD8+ and CD4+ T cells. Class I heavy chain molecules are represented in this study by both the ubiquitously expressed classical HLAs A and C, and the more restricted nonclassical HLAs F and G. Heavy chains associate with the constant light chain molecule  $\beta$ 2-microglobulin, increases of which in cerebrospinal fluid correspond to the level of neuroAIDS.<sup>22</sup> Class II MHC molecules include HLA-DR $\beta$ 1 and Ia-associated  $\gamma$ -chain/CD74. Accessory genes involved in antigen processing, such as those involved in proteosomal protein degradation, including PA28 $\alpha$  and - $\beta$ , and PSMB8 and PSMB9, are also induced in SIVE.

### *Lysosomal Proteins*

Lysosomes break down intracellular molecules crucial for multiple cellular functions including antigen presentation. Interestingly, many of the up-regulated genes are lysosome-associated molecules. The association of increased lysosomal hydrolytic enzyme activity with HIV CNS infection has been reported;<sup>23</sup> we similarly find proteases such as cathepsin A and H to be up-regulated. Furthermore, other lysosomal proteins, such as LAPTMs, a factor in lysosomal membrane dynamics that is associated with microglia activation after neuronal apoptosis,<sup>24</sup> are up-regulated, indicating additional lysosomal

processes that may be involved in escalating the damage of neuroAIDS.

### *Interferon-Inducible*

#### *Genes/Antiviral/Transcriptional Regulation*

More than 300 IFN-inducible genes have been identified and the proteins encoded by these genes play a large part in the antiviral response. Induction of many of the IFN-inducible genes, including MxA, adenosine deaminase, and 2-5 oligoadenylate synthase (2-5OA) can lead to actions protective against many viruses including, for 2-5OA, protection from HIV infection.<sup>25</sup>

Transcription of these genes after stimulation of IFN $\alpha/\beta$  or  $\gamma$  receptors leads to the phosphorylation of signal transducer and activator of transcription (STAT)1 $\alpha/\beta$  homodimers or of heterodimers in association with STAT2. On activation, the STAT molecules, which can also complex with p48protein/ISGF3 $\gamma$ , are translocated to the nucleus to stimulate transcription of genes including Mac-binding protein, ISG12, ISG15, and GIP3.

A transcriptional activator found up-regulated in activated and differentiated macrophages is nuclear factor interleukin 6 (NF-IL6), which is essential for HIV-1 replication in these cells.<sup>26</sup> This molecule is also involved in the gene expression of several inflammatory cytokines in conjunction with STAT3.

### *Cell Cycle and Growth, Differentiation, and Signaling*

Cell proliferation, such as the astro- and microgliosis seen in SIVE/HIVE cases, involves up-regulation of cell-cycle elements, along with cell growth and differentiation. Cell-cycle progression relies on the effects of cyclins, such as cyclin D3, on the activity of cyclin-dependent protein kinases to enable the transcription of genes required in S phase of the cell cycle.

Epithelin/granulin peptides are growth factors for dividing cells, as is the cytokine midkine, which is involved in neuronal development, growth, and maintenance. Activation of fibroblast growth factor receptor-1, or CD81/target of anti-proliferative antibody 1 (TAPA1), can also increase cell proliferation rates, especially in angiogenesis and astrocytosis.

### *Cytoskeleton*

Cell changes in neuroAIDS can include alterations in cell size and shape. Examples are the increased expression of intermediate filaments including, in astrocytes, vimentin which can alter cell shape and process length by association with plectin at the cell membrane. Plectin also binds GFAP, actin, and integrin- $\beta$ 4. Additionally, vimentin has a close relationship to CapG/macrophage capping protein, moesin, and actin, with the assembly of the latter involving the GTPase RhoG, a participant in neurite outgrowth.

### *Immune System*

Some of the up-regulated genes are important in cells of the immune system. Of note, CapG (see also Cytoskeleton) accounts for 1% of the total protein in macrophages. CD14 and CD163 are specific markers for these cells and are more highly expressed in activated macrophages during inflammatory reactions, as is human cartilage glycoprotein 39 (HCgp39). Glut5, a fructose transporter with unknown CNS function, is expressed in resting and up-regulated microglia.<sup>27</sup> Moreover, the enzyme ribonuclease K6 resides in monocytes and neutrophils.

### *Other Brain Regions*

Tissue RNA was also available from three other brain areas: the occipital lobe, the midbrain, and cerebellum from selected animals (at least four SIVE and three controls for each location). GeneChip analysis was performed to examine the expression levels of the genes found to be up-regulated in the frontal lobe samples. As indicated in Table 2, 66 of the 98 genes were also up-regulated in the occipital lobe, with 68 in the midbrain and 19 in the cerebellum. All brain regions examined had genes that were predominant in the *Interferon Inducible* and *Antigen Presentation* categories. The cerebellum showed little up-regulation of genes in the other categories, suggesting that, in this model, there is far less involvement of this part of the brain. Interestingly there was little representation of the frontal lobe up-regulated genes from the *Cytoskeleton* and *Growth and Differentiation* categories in the other three brain regions, suggesting that cellular reorganization is a higher factor in the frontal lobe.

### *Infiltrating Macrophages and Parenchymal Microglia Express Many of the Up-Regulated Genes*

Tissue samples taken for our RNA analysis contain the whole array of CNS cells such as neurons, oligodendrocytes, astrocytes, microglia, and endothelial cells, as well as cells found within lesions associated with SIV infection, such as infiltrating macrophages and lymphoid cells, and MNGCs. Certainly, analyzing gene array provides an overview of up-regulated genes in whole tissue, but of equal importance is pinpointing the specific locations of these genes' products. Furthermore, up-regulation of RNA may not necessarily correspond to that of the protein product. To assess up-regulation of protein, and to gain insight into the cellular origin of the up-regulated genes, serial sections of frontal lobe from SIVE and uninfected control monkeys were immunostained with antibodies corresponding to 14 of the up-regulated genes, chosen to represent the functional groups described above. Subsequent immunohistochemical staining for GFAP (astrocytes), HAM56 (macrophages and activated microglia), and LCA (lymphocytes) then aided identification of affected cells. Two additional genes, HCgp39 and

ISG12, were examined at the RNA level by *in situ* hybridization.

Most of the immunoreactivity and *in situ* hybridization signals occurred within the SIVE lesions, including perivascular cuffs and microglia/macrophage nodules. Such lesions were predominately composed of HAM56-positive microglia/macrophages (Figure 1A) with LCA staining of three to four lymphocytes (Figure 1B), and with GFAP-reactive astrocytes surrounding, but rarely infiltrating, many of the nodular lesions (Figure 1C). Within the lesions, staining was intense for CD163 (Figure 1D), Glut5 (Figure 1E), HLA-DR (Figure 1F), tTG (Figure 1G), and vimentin (Figure 1H). HCgp39 (see below, Figure 3A) and ISG12 *in situ* hybridization revealed signal over nodules of macrophages. Immunohistochemistry further revealed that ACT showed strong localization to large cells where foamy macrophages appeared (Figure 1I). STAT1 and C1q (Figure 1J) were also found in these nodules, but to a lesser degree. ApoD (Figure 1K), CD37 (Figure 1L), and cyclin D3 were each found in only two or three distinct cells in lesions. MNGCs were not uniformly stained with these antibodies. HLA-DR (Figure 1M), tTG (see Figure 1G), vimentin (Figure 1N), and HAM56 produced a very dark reaction product in MNGCs (including, with vimentin, an even darker central area); whereas C1q, CD163, Glut5, and ACT (Figure 1O) showed much lighter staining.

In parenchymal microglia from the SIVE cases, CD163 (Figure 2A, see also Figure 1D) was induced, and Glut5 (Figure 2C, see also Figure 1E) clearly increased compared to amounts in uninfected controls (Figure 2, B and D, respectively). HLA-DR (see Figure 1, F and M) occupied white matter microglia in concordance with HAM56 (Figure 2E), but neither of these was identified in parenchymal microglia of uninfected controls (eg, Figure 2F; HLA-DR). Less frequently, microglia expressing ACT, C1q, STAT1, and tTG (Figure 2G) could be found, predominantly around lesions. Control tissue had no C1q or STAT1 at all, and tTG was found only along the endothelium (Figure 2H).

### *Neurons and Other Native CNS Cells from SIV-Infected Animals Express a Wide Array of Novel Proteins*

In addition to microglia, other native cells of the CNS also displayed induction or increased expression of markers. In SIV-infected brains, the HCgp39 signal appeared in white matter (Figure 3A), in the vicinity of lesions and occasionally in patches along the white/gray matter junction; in controls, only a few isolated white matter cells contained HCgp39 (Figure 3B). Although HCgp39 was found in macrophages in the lesions, the strongest signal was predominately found in cells that did not react with HAM56. Similarly ISG12 was also found in cells that did not stain with HAM56 (data not shown). In both cases these cells are presumably astrocytes but staining for GFAP was not performed in conjunction with *in situ* hybridization. Cells with clear astrocytic morphology expressed tTG, vimentin (Figures 1, H and N), ACT, STAT1

(Figure 3C), and ISG15 (Figure 3E). Of these, ACT stained only occasional astrocyte patches in control tissue, whereas neither ISG15 nor STAT1 (Figure 3D) reacted at all with astrocytes in controls.

Endothelial cells in the brains of animals with SIVE expressed vimentin (Figure 1N), tTG (Figure 2G), ACT, ApoD, and STAT1 (Figure 3C) throughout the vascular endothelium in the setting of SIV-induced CNS pathology. Expression of vWf was much stronger (Figure 3G) than in the controls (Figure 3H), and similarly a moderate level of CD31 (Figure 3F) was found in the SIVE cases compared to only faint staining in control cases.

The cytoplasm of distinct swaths of neurons located in cortical layers 4 to 6 were notably stained with ACT (Figure 4A), whereas cyclin D3 (Figure 4C) was highly expressed in the nuclei of numerous neurons in cortical layers 3 to 6, and tTG (Figure 4E) was also encountered in many neuronal nuclei. This pattern occurred in all neurons of some areas but, elsewhere, only those in distinct layers or occasional cells. STAT1 stained unique, individual neurons, mostly classed as large pyramidal cells (Figure 4F). None of these antibodies stained neurons in control tissue (ACT, Figure 4B; cyclin D3, Figure 4D; tTG, Figure 2H).

In addition to examining brains from uninfected, untreated monkeys, two additional sets of controls were performed. First, two of the uninfected animals received the CD8+ cell-depletion protocol. These were indistinguishable from the other four controls as to expression of the identified genes on the array analysis (data not shown); they did not exhibit neuropathological changes at necropsy, and their immunohistochemical analysis was consistent with that of the other controls (not shown). Second, brain sections from two animals that developed SIVE after a natural course of SIV infection (no CD8+ cell depletion; development of simian AIDS at an average of 11 months after infection) were examined by immunohistochemical staining for all of the protein markers. For all, the pattern of staining was consistent with that seen in animals with rapid SIVE induced by the CD8 depletion protocol (eg, Figure 5; A to F).

### *Discussion*

Microarray analysis was used to investigate mRNA abundance in the frontal lobes of rhesus macaques with SIVE compared to that in uninfected monkeys. Statistical analysis revealed 98 up-regulated genes, the majority of which have never before been described in SIVE cases. Many of these were confirmed and localized to specific cell types within the brain at the protein and RNA level by the techniques of immunohistochemistry and *in situ* hybridization. As our results show, we identified an ensemble of genes and proteins up-regulated in association with SIVE and classified them into categories that reflect the following pathogenic processes thought responsible for neuroAIDS: monocyte entry into the brain; production of neurotoxic effectors; transcription factors that alter CNS gene expression; and signature markers of activated astrocytes, endothelial cells, macrophages, and



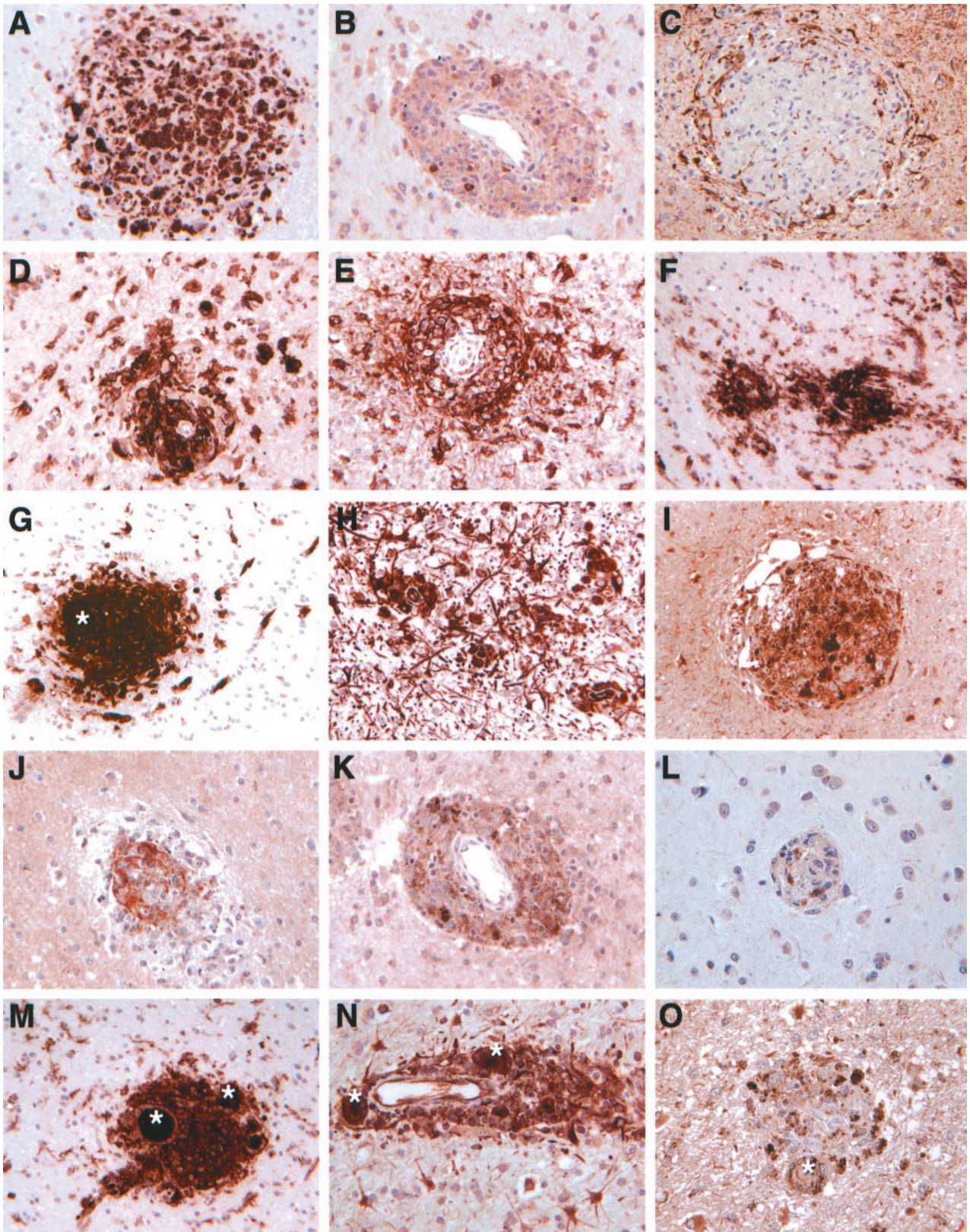


**Figure 1.** Immunohistochemical staining of cellular infiltrates in SIVE revealing HAM56-positive microglia/macrophages in nodule (A) and LCA-positive lymphocytes contributing to a perivascular infiltrate (B). C: GFAP-positive astrocytes surround a nodule. Immunoreactivity is also found for CD163 (D), Glut5 (E), HLA-DR (F), tissue transglutaminase (TG) (G), vimentin (H),  $\alpha$ 1-anti-chymotrypsin (ACT) (I), C1q (J), apolipoprotein D (K), and CD37 (L). Reactivity of MNGCs varies, as shown for HLA-DR (M), vimentin (N), and ACT (O). Asterisk indicates MNGCs.

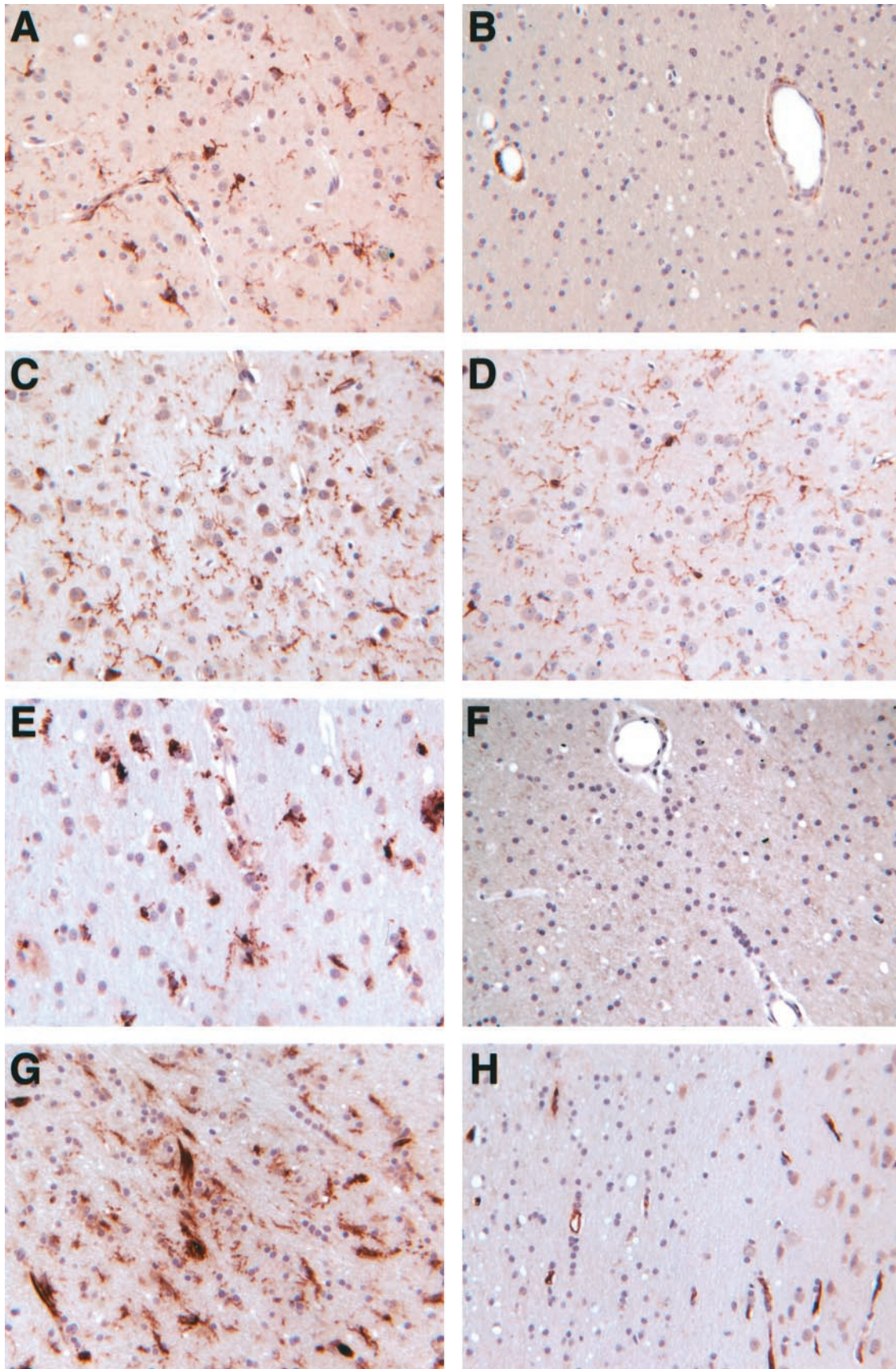


**Figure 2.** Immunohistochemical staining of parenchymal microglia in SIV-induced CNS pathology and control brains, respectively, using CD163 (**A, B**), Glut5 (**C, D**), HAM56/HLA-DR (**E, F**), and tTG (**G, H**).

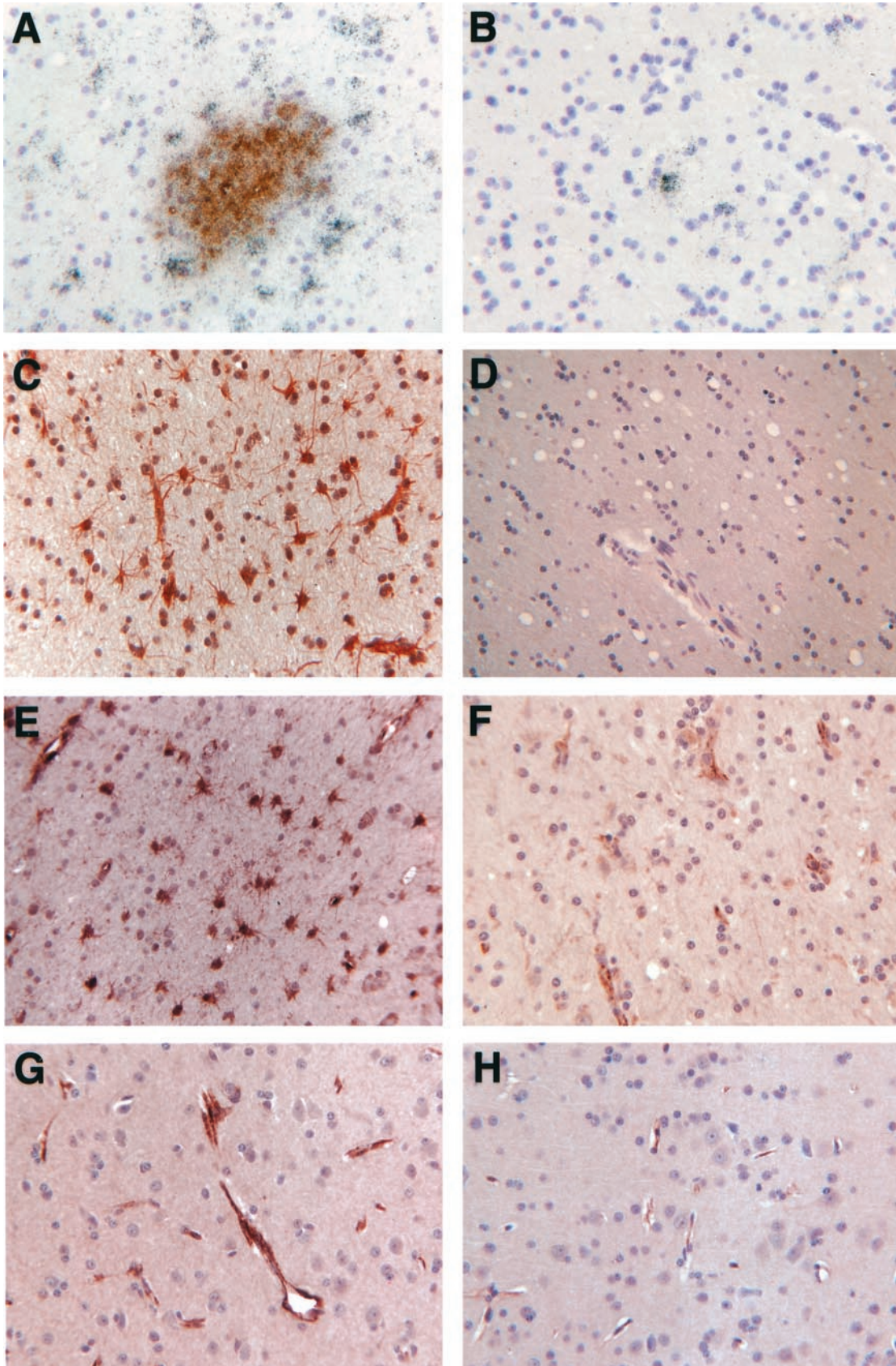


**Figure 3.** A and B: Glial reactivity for HCgp39 (*in situ* hybridization, combined with immunohistochemistry for HAM56 (A, SIVE; B, control). C and D: Immunohistochemical staining for STAT1 (C, SIVE; D, control) and ISG15 (E, SIVE). Endothelial reactivity in immunohistochemical staining for CD31 in SIVE (F) and von Willebrand factor (vWF) in SIVE (G) and control (H) brains.

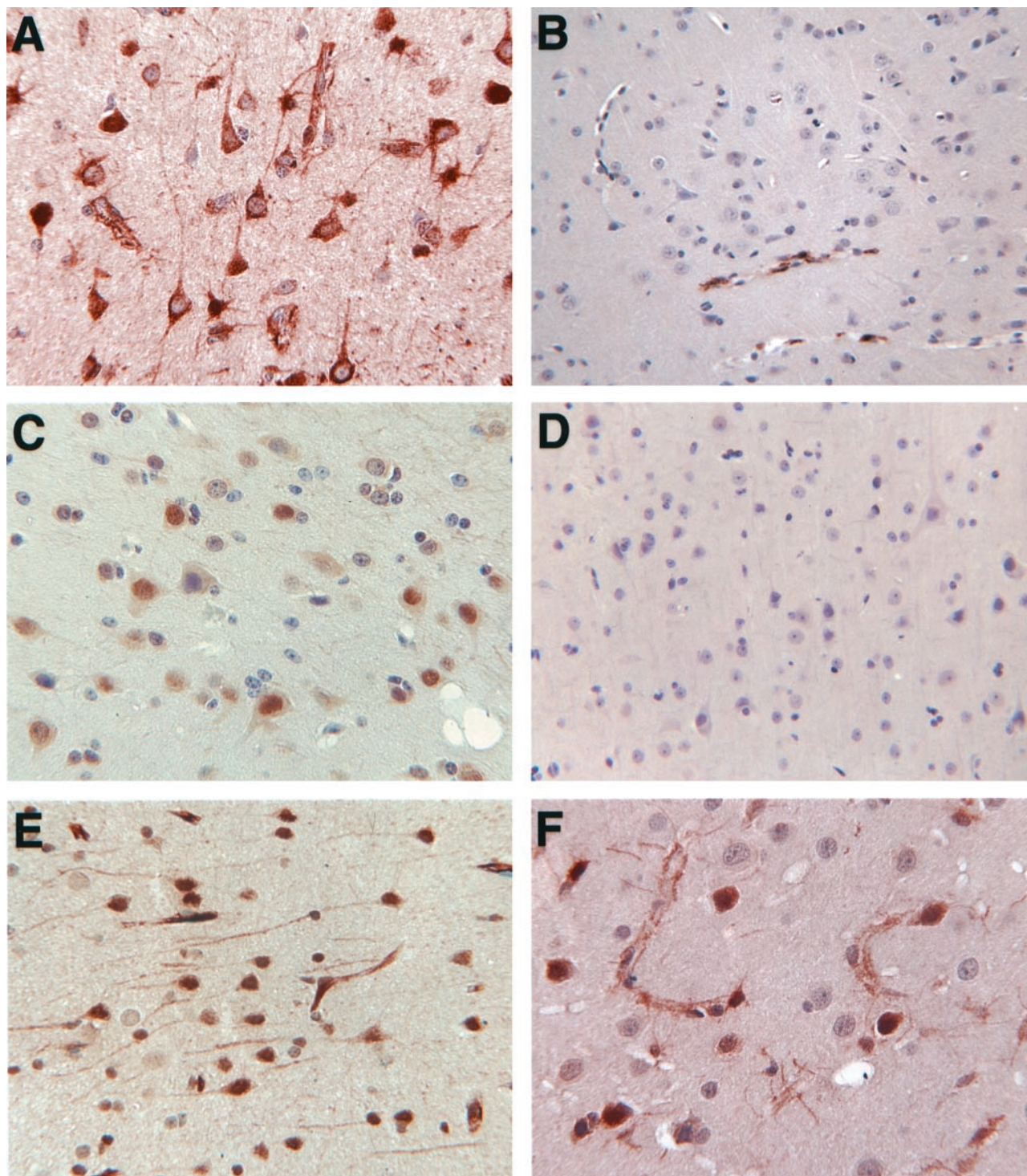


**Figure 4.** Immunohistochemical reactivity in neurons for ACT (**A**, SIVE, also showing astrocyte reactivity; **B**, control), cyclin D3 (**C**, SIVE; **D**, control), tTG in SIVE (**E**), and STAT1 in SIVE (**F**).

microglia. Furthermore, finding induction of genes and their protein products within cortical neurons points to specific neuronal responses to SIVE, including those linked to apoptotic pathways. Although this technology has been applied to several other CNS disorders including multiple sclerosis, schizophrenia, and brain tumors,

this is the first investigation of CNS disease induced by immunodeficiency virus infection.

NeuroAIDS is thought to develop after increased CNS invasion by infected and activated macrophages which, in turn, leads to up-regulation of resident microglia as well as of astrocytes, leading to damage in the CNS environ-

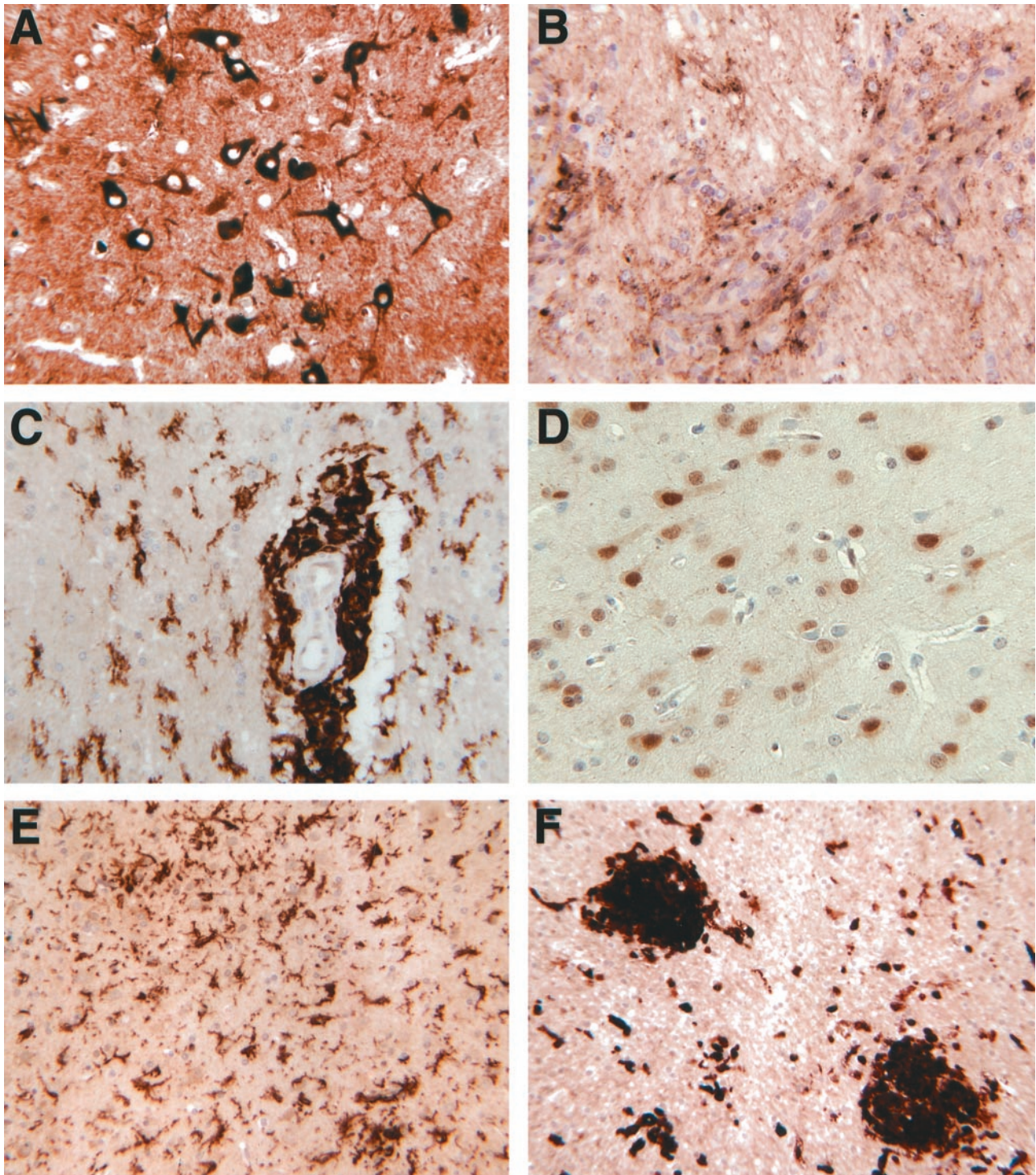


**Figure 5.** Immunohistochemical staining of brains from SIV-infected animals developing spontaneous SIVE. **A**, ACT in neurons; **B**, ApoD in perivascular and infiltrating cells; **C**, CD163 in perivascular macrophages and parenchymal microglia; **D**, cyclin D3 in neurons; **E**, Glut5 in parenchymal microglia; and **F**, tTG in nodules and infiltrating and/or parenchymal cells.

ment causing neuronal injury and loss. One of the key histological and pathogenic features of neuroAIDS is increased monocyte entry into the brain, and we found a number of genes in the SIVE cases connected to this process. Migration of monocytes through endothelial cells is dependent on both cell types expressing CD31 and CD99; and CD99 itself plays a crucial role in mono-

cyte diapedesis,<sup>10</sup> the transendothelial migration in which the monocyte crosses the blood-brain barrier and becomes a brain macrophage. CD99 is also implicated in cell aggregation<sup>28</sup> and thus may be involved both in the recruitment of monocytes to, and formation of, macrophage/microglia nodules in SIVE/HIVE. Monocyte migration is also aided by tissue transglutaminase (tTG),<sup>12</sup>

which we found prominently expressed on endothelial cells as well as on macrophages/microglia. Osteopontin is a multifunctional molecule with potent chemotactic and haptotactic actions on monocytes<sup>13,29</sup> and can also contribute to monocyte recruitment and CNS pathology. Interestingly, transcript sequencing from human multiple sclerosis plaques revealed abundant transcripts for osteopontin, and microarray analysis of spinal cord RNA from rats with experimental autoimmune encephalomyelitis (EAE), a mouse model for multiple sclerosis, revealed increased levels of osteopontin.<sup>30</sup> Furthermore, microarray analysis of brain RNA from mouse models of Huntington's disease and from patients with Huntington's disease also revealed increased levels of osteopontin.<sup>31</sup> In addition to its effects on monocytes, pleiotropic osteopontin may play additional roles in these CNS inflammatory and degenerative diseases.

The enhanced expression of these genes and proteins demonstrated here reinforces theories of damage occurring to the CNS after changes to the blood-brain barrier and a related surge of monocyte entry. In SIV- and HIV-induced CNS disease, analysis of the factors promoting monocyte migration has predominantly focused on the ICAM-1 and VCAM adhesion molecules and MCP-1, RANTES, and IP-10 chemokines, however these may be insufficient to explain macrophage accumulation in the CNS in neuroAIDS.<sup>32</sup> We now present CD99, tTG, and osteopontin as new candidate effectors in the monocyte accumulation found in SIV- and HIV-induced CNS disease. These molecules and the mechanisms through which they act can provide invaluable guides for therapy that aims at arresting monocyte migration into the brain and decreasing CNS inflammation.

Cells of the macrophage lineage are key to the pathogenesis of neuroAIDS as this condition correlates closely with the degree of microglia/macrophage activation.<sup>1</sup> Neuronal dysfunction and loss in patients with AIDS has been attributed to the increased release of potentially toxic factors from the large number of infiltrating macrophages as well as activated microglia and astrocytes. Activated microglia in the white matter were notable here for expression of HLA-DR, CD163, and Glut5. Although the function of Glut5 in the CNS is unknown, as it has previously only been characterized as a fructose transporter, CD163 receptor activation is involved in the secretion of IL1 $\beta$ , IL6, and GM-CSF, increases of which occur in the brains of HIV+ patients and have been linked to pathological mechanisms.<sup>33,34</sup>

We have also observed the increased expression of Glut5 and CD163 associated with ramified, gray matter microglia. This outcome denotes a much more widespread up-regulation of resident microglia than previously thought, in fact extending beyond those surrounding infected cells. This generalized spread could contribute to the more subtle neuronal damage, such as dendritic and synaptic changes, in SIV-infected animals and HIV-infected patients. Considering their ability to stain such a diverse microglial population, CD163 and especially Glut5 may be more sensitive markers than the commonly used HLA-DR and HAM56 for examining microglia activation in diverse clinical diseases.

Interestingly, microarray analysis of genes induced by exposure of monocyte-derived macrophages to the HIV gp120 surface protein did not produce similar genes to those found in our study.<sup>35</sup> This implies that direct effects of gp120 on cells of the monocyte lineage in the brain is not sufficient to induce the pathological cascade resulting in neuroAIDS. Furthermore, although isolating and analyzing individual components of a response is an invaluable part of pathogenic assessment, the interactions between these parts can be more complex than the sum, and studies in the brain and other organs can necessitate the use of tissue containing all of the interacting components.

Astrogliosis can also accompany neuroAIDS, and many of the genes identified here can be linked to this process, including changes in astrocyte shape and activation state. Astrocytes in the vicinity of lesions were shown to express Clq, tTG, vimentin, and HCgp39; while  $\alpha$ 1-anti-chymotrypsin (ACT), STAT1, and ISG15 also stained a more diffuse set of astrocytes. ACT has a role in many processes including regulation of inflammation, apoptosis, complement activation, and viral pathogenesis.<sup>36</sup> Many reports cite astrocytes as the main ACT-expressing cell after any sort of CNS inflammation. ACT is also expressed in  $\beta$ -APP-containing plaques in brains of patients with Alzheimer's disease,<sup>37</sup> and reciprocally  $\beta$ -APP has been found to be present in HIVE-associated lesions,<sup>38</sup> although the characteristic Alzheimer's plaques are not present in HIV-induced dementia.

Another significant finding in astrocytes of SIV-infected brains is STAT1, which is not only up-regulated by IFNs<sup>39</sup> but also acts as a signal transducer for these cytokines, leading to the up-regulation of many IFN-inducible genes such as ISG15 and others found in this study. Many of these have anti-viral activity, both for the well-known molecules like 2-5OA and less characterized ones including ISG12 investigated here, which has been recently shown to be protective in lethal mouse Sinbis virus encephalitis.<sup>40</sup> Similar up-regulation of IFN-induced genes have been found in microarray analyses of other viral infections including hepatitis C virus infection of the chimpanzee liver,<sup>41</sup> human cytomegalovirus infection of fibroblasts,<sup>42</sup> and hantavirus infection of endothelial cells.<sup>43</sup>

The CNS function of some of these up-regulated genes/proteins can be linked to pathogenic processes. For example tTG is known to be involved in apoptosis<sup>44</sup> and was previously reported to be highly up-regulated in MNGCs and lesions in HIVE.<sup>45</sup> An intriguing finding was the up-regulation of SPPL2b/PSL1 (presenilin-like protein 1). This is a member of the signal peptide peptidase family of intramembrane proteases<sup>16</sup> that is similar to the presenilins, thought to be crucial in Alzheimer's disease pathogenesis. The product of another gene, VDUP1/TBP-2 (thioredoxin-binding protein-2) lowers the thiol-reducing activity and level of expression of thioredoxin.<sup>46</sup> This can lead to an accumulation of reactive oxygen species and resultant oxidative stress damage, including induction of apoptosis.<sup>47</sup> Thus these comprise other candidate mechanisms of neuronal damage in neuroAIDS.

The induction of another inflammatory protein, indoleamine 2,3-dioxygenase (IDO), is a critical step lead-

ing to production of the excitatory neurotoxin quinolinic acid, the presence of which in the CNS correlates with the severity of CNS dysfunction and cerebral volume loss resulting from HIV infection.<sup>14,48</sup> We have recently confirmed the strong up-regulation of IDO mRNA in these SIV-infected brains by real-time reverse transcriptase-polymerase chain reaction and found that IDO is expressed by macrophages within nodules.<sup>49</sup> An additional likely mediator of CNS damage is tissue plasminogen activator (tPA). Although best characterized for its lysis of blood clots, tPA's release from neurons and microglia leads to microglial activation, and both excitotoxin-induced seizures and neuronal death are dependent on tPA production.<sup>15,50</sup> Thus, the mechanisms that underlie inflammation in neuroAIDS are found among other CNS diseases and represent excellent potential targets in future treatment paradigms.

Our immunohistochemical analysis was especially valuable for localizing up-regulation of protein products to neurons including STAT1, tTG, ACT, and cyclin D3, all novel findings with implications for pathogenesis. Neuronal STAT1 similarly increases in EAE<sup>51</sup> and, *in vitro*, STAT1 is linked to dendritic retraction after IFN- $\gamma$  stimulation.<sup>52</sup> Such a mechanism of dendritic injury may be partially responsible for that accompanying cognitive dysfunction in patients with neuroAIDS.<sup>2</sup> TTG expression in neurons *in vitro* has been shown to lead to increased cellular oxidative stress, sensitizing them to apoptosis.<sup>53</sup> Furthermore, tTG expression in neurons *in vivo* has been strongly implicated in the damage found in Huntington's disease.<sup>31,54</sup> In support of this, administration of cystamine, a competitive inhibitor to tTG, ameliorates pathology in mouse models of Huntington's disease<sup>31,55</sup> and thus may represent an important direction of study for SIVE/HIVE cases. Although its function is unknown, neuronal ACT has been found to be up-regulated in the brainstem of people with spinocerebellar ataxia type 1, like Huntington's, a CAG-trinucleotide repeat (polyglutamine) neurodegenerative disorder.<sup>56</sup>

Cyclin D3, which is involved in the cell-cycle control system, is of particular interest here. Immunostaining for cyclin D3 located it predominately in the nuclei of neurons in cortical layers 3 to 6. Cyclin D3 can phosphorylate the cell-cycle regulator Rb during G<sub>1</sub> phase allowing the release of the protein E2F1.<sup>57</sup> Although the normal function of E2F1 is to activate the gene expression needed for cell-cycle progression,<sup>58</sup> increased amounts of E2F1 in postmitotic cells such as neurons can also result in apoptosis.<sup>59</sup> In addition, neuronal death can be attributed in part to pRb phosphorylation itself,<sup>60</sup> and an increased and altered expression of the phosphorylated form of pRb exists in neuronal populations of HIVE- and SIVE-affected brains.<sup>61,62</sup> These latter studies, like ours, documented a predominantly nuclear staining of cell-cycle regulatory proteins, suggesting that the up-regulation of cyclin D3 found here is a precursor to increased pRb phosphorylation, E2F1 release, and neuronal death. In addition cyclin D3 can directly interact with caspase-2, resulting in an increase in the apoptosis-inducing, cleaved form of this molecule.<sup>63</sup> In fact, a cascade of neuronal caspase activation underlies dendritic degen-

eration and neuronal apoptosis in models of HIV neurotoxicity.<sup>64</sup>

Neuronal damage has been hypothesized to occur *in vivo* during HIV infection because of the production and release of toxins by infected and/or activated microglia/macrophages. In the frontal lobes of SIV-infected animals studied here, the macrophage-containing lesions were predominately in the white matter, where microglial activation markers were also pronounced and astrocytes became activated. Therefore, a noteworthy observation is that the up-regulated neuronal proteins found here (cyclin D3, ACT, tTG, and STAT1) were located primarily in neurons from cortical layer 3 inward, suggesting that the proximity of these neurons to the source of damaging molecules is a key factor in neuronal pathogenesis. Indeed, Golgi impregnation staining has revealed significant damage to cortical neuronal dendrites in these SIV-infected animals (RF Mervis and HS Fox, unpublished data). Thus, it is indeed likely that products of infected and/or activated macrophages, such as those identified here, potentially amplified by additional factors from locally activated astrocytes and microglia, lead to untoward effects on neurons resulting in neuroAIDS.

In conclusion, this study has highlighted a number of novel genes and proteins, identified through unbiased assessment of gene expression levels by microarray analysis, that have not been previously considered in this field. These data support the role of activated macrophages and microglia in the injurious effects of HIV on the CNS, identify an upstream factor in the cell cycle-related abnormalities found in SIVE/HIVE neurons, and reveal molecular pathways whose modulation can potentially reduce cellular infiltration and neuronal dysfunction in those suffering from these devastating consequences of HIV infection of the CNS.

### Acknowledgments

We thank Drs. Keith Reimann and Jörn Schmitz for their assistance and input into the CD8-depletion protocol; Dr. Ernest Borden for ISG15 antisera; Steve Head, Jeff Chismar, Tom Whisenant, and Tony Mondala for their valuable expertise in microarray experiments; Rebecca Mahady for manuscript preparation; and the authors of all of the publications not able to be included as references in this article because of the sheer numbers needed for investigation of all of the genes of interest.

### References

1. Glass JD, Fedor H, Wesselingh SL, McArthur JC: Immunocytochemical quantitation of human immunodeficiency virus in the brain: correlations with dementia. *Ann Neurol* 1995, 38:755-762
2. Masliah E, Heaton RK, Marcotte TD, Ellis RJ, Wiley CA, Mallory M, Achim CL, McCutchan JA, Nelson JA, Atkinson JH, Grant I: Dendritic injury is a pathological substrate for human immunodeficiency virus-related cognitive disorders. HNRC Group. The HIV Neurobehavioral Research Center. *Ann Neurol* 1997, 42:963-972

3. Burudi EME, Fox HS: Simian immunodeficiency virus model of HIV-induced central nervous system dysfunction. *Advances in Virus Research*. Edited by MJ Buchmeier, I Campbell. Academic Press, 2001, pp 431–464
4. Zink MC, Spelman JP, Robinson RB, Clements JE: SIV infection of macaques—modeling the progression to AIDS dementia. *J Neurovirology* 1998, 4:249–259
5. Schmitz JE, Kuroda MJ, Santra S, Sasseville VG, Simon MA, Lifton MA, Racz P, Tenner-Racz K, Dalesandro M, Scallon BJ, Ghayeb J, Forman MA, Montefiori DC, Rieber EP, Letvin NL, Reimann KA: Control of viremia in simian immunodeficiency virus infection by CD8+ lymphocytes. *Science* 1999, 283:857–860
6. Williams K, Alvarez X, Lackner AA: Central nervous system perivascular cells are immunoregulatory cells that connect the CNS with the peripheral immune system. *Glia* 2001, 36:156–164
7. Kaul M, Garden GA, Lipton SA: Pathways to neuronal injury and apoptosis in HIV-associated dementia. *Nature* 2001, 410:988–994
8. Chismar JD, Mondala T, Fox HS, Roberts E, Langford D, Masliah E, Salomon DR, Head SR: Analysis of result variability from high-density oligonucleotide arrays comparing same-species and cross-species hybridizations. *Biotechniques* 2002, 33:516–524
9. Kayo T, Allison DB, Weindruch R, Prolla TA: Influences of aging and caloric restriction on the transcriptional profile of skeletal muscle from rhesus monkeys. *Proc Natl Acad Sci USA* 2001, 98:5093–5098
10. Schenkel AR, Mamdouh Z, Chen X, Liebman RM, Muller WA: CD99 plays a major role in the migration of monocytes through endothelial junctions. *Nat Immunol* 2002, 14:143–150
11. Wenzel I, Roth J, Sorg C: Identification of a novel surface molecule, RM3/1, that contributes to the adhesion of glucocorticoid-induced human monocytes to endothelial cells. *Eur J Immunol* 1996, 26:2758–2763
12. Akimov SS, Belkin AM: Cell surface tissue transglutaminase is involved in adhesion and migration of monocytic cells on fibronectin. *Blood* 2001, 98:1567–1576
13. Giachelli CM, Lombardi D, Johnson RJ, Murry CE, Almeida M: Evidence for a role of osteopontin in macrophage infiltration in response to pathological stimuli in vivo. *Am J Pathol* 1998, 152:353–358
14. Heyes MP, Saito K, Lackner A, Wiley CA, Achim CL, Markey SP: Sources of the neurotoxin quinolinic acid in the brain of HIV-1-infected patients and retrovirus-infected macaques. *EMBO J* 1998, 12:881–896
15. Tsirka SE, Gualandris A, Amaral DG, Strickland S: Excitotoxin-induced neuronal degeneration and seizure are mediated by tissue plasminogen activator. *Nature* 1995, 377:340–344
16. Weihofen A, Binns K, Lemberg MK, Ashman K, Martoglio B: Identification of signal peptide peptidase, a presenilin-type aspartic protease. *Science* 2002, 296:2215–2218
17. Belloir B, Kovari E, Surini-Demiri M, Savioz A: Altered apolipoprotein D expression in the brain of patients with Alzheimer disease. *J Neurosci Res* 2001, 64:61–69
18. Terrisse L, Poirier J, Bertrand P, Merched A, Visvikis S, Siest G, Milne R, Rassart E: Increased levels of apolipoprotein D in cerebrospinal fluid and hippocampus of Alzheimer's patients. *J Neurochem* 1998, 71:1643–1650
19. Aukrust P, Bjornsen S, Lunden B, Otterdal K, Ng EC, Ameln W, Ueland T, Muller F, Solum NO, Brosstad F, Froland SS: Persistently elevated levels of von Willebrand factor antigen in HIV infection. Downregulation during highly active antiretroviral therapy. *Thromb Haemost* 2000, 84:183–187
20. Gollin PA, Kalaria RN, Eikelenboom P, Rozemuller A, Perry G: Alpha 1-antitrypsin and alpha 1-antichymotrypsin are in the lesions of Alzheimer's disease. *Neuroreport* 1992, 3:201–203
21. Tooyama I, Sato H, Yasuhara O, Kimura H, Konishi Y, Shen Y, Walker DG, Beach TG, Sue LI, Rogers J: Correlation of the expression level of C1q mRNA and the number of C1q-positive plaques in the Alzheimer disease temporal cortex. analysis of C1q mRNA and its protein using adjacent or nearby sections. *Dement Geriatr Cogn Disord* 2001, 12:237–242
22. McArthur JC, McClernon DR, Cronin MF, Nance-Sproson TE, Saah AJ, St Clair M, Lanier ER: Relationship between human immunodeficiency virus-associated dementia and viral load in cerebrospinal fluid and brain. *Ann Neurol* 1997, 42:689–698
23. Gelman BB, Wolf DA, Rodriguez-Wolf M, West AB, Haque AK, Cloyd M: Mononuclear phagocyte hydrolytic enzyme activity associated with cerebral HIV-1 infection. *Am J Pathol* 1997, 151:1437–1446
24. Origasa M, Tanaka S, Suzuki K, Tone S, Lim B, Koike T: Activation of a novel microglial gene encoding a lysosomal membrane protein in response to neuronal apoptosis. *Brain Res Mol Brain Res* 2001, 88:1–13
25. Schroeder HC, Ugarkovic D, Merz H, Kuchino Y, Okamoto T, Muller WE: Protection of HeLa-T4+ cells against human immunodeficiency virus (HIV) infection after stable transfection with HIV LTR-2', 5'-oligoadenylate synthetase hybrid gene. *EMBO J* 1990, 4:3124–3130
26. Henderson AJ, Connor RI, Calame KL: C/EBP activators are required for HIV-1 replication and proviral induction in monocytic cell lines. *Immunity* 1996, 5:91–101
27. Payne J, Maher F, Simpson I, Mattice L, Davies P: Glucose transporter Glut 5 expression in microglial cells. *Glia* 1997, 21:327–331
28. Bernard G, Raimondi V, Alberti I, Pourteim M, Widjenes J, Ticchioni M, Bernard A: CD99 (E2) up-regulates alpha4beta1-dependent T cell adhesion to inflamed vascular endothelium under flow conditions. *Eur J Immunol* 2000, 30:3061–3065
29. Weber GF, Zawaideh S, Hikita S, Kumar VA, Cantor H, Ashkar S: Phosphorylation-dependent interaction of osteopontin with its receptors regulates macrophage migration and activation. *J Leukoc Biol* 2002, 72:752–761
30. Chabas D, Baranzini SE, Mitchell D, Bernard CC, Rittling SR, Denhardt DT, Sobel RA, Lock C, Karpuj M, Pedotti R, Heller R, Oksenberg JR, Steinman L: The influence of the proinflammatory cytokine, osteopontin, on autoimmune demyelinating disease. *Science* 2001, 294:1731–1735
31. Karpuj MV, Becher MW, Springer JE, Chabas D, Youssef S, Pedotti R, Mitchell D, Steinman L: Prolonged survival and decreased abnormal movements in transgenic model of Huntington disease, with administration of the transglutaminase inhibitor cystamine. *Nat Med* 2002, 8:143–149
32. Williams KC, Hickey WF: Central nervous system damage, monocytes and macrophages, and neurological disorders in AIDS. *Annu Rev Neurosci* 2002, 25:537–562
33. Benveniste EN: Cytokine circuits in brain. Implications for AIDS dementia complex. *Res Publ Assoc Res Nerv Ment Dis* 1994, 72:71–88
34. Van den Heuvel MM, Tensen CP, van As JH, Van den Berg TK, Fluitsma DM, Dijkstra CD, Dopp EA, Droste A, Van Gaalen FA, Sorg C, Hogger P, Beelen RH: Regulation of CD 163 on human macrophages: cross-linking of CD163 induces signaling and activation. *J Leukoc Biol* 1999, 66:858–866
35. Cicala C, Arthos J, Selig SM, Dennis G, Jr., Hosack DA, Van Ryk D, Spangler ML, Steenbeke TD, Khazanie P, Gupta N, Yang J, Daucher M, Lempicki RA, Fauci AS: HIV envelope induces a cascade of cell signals in non-proliferating target cells that favor virus replication. *Proc Natl Acad Sci USA* 2002, 99:9380–9385
36. Janciauskiene S: Conformational properties of serine proteinase inhibitors (serpins) confer multiple pathophysiological roles. *Biochim Biophys Acta* 2001, 1535:221–235
37. Pasternack JM, Abraham CR, Van Dyke BJ, Potter H, Younkin SG: Astrocytes in Alzheimer's disease gray matter express alpha 1-antichymotrypsin mRNA. *Am J Pathol* 1989, 135:827–834
38. Nebuloni M, Pellegrinelli A, Ferri A, Bonetto S, Boldorini R, Vago L, Grassi MP, Costanzi G: Beta amyloid precursor protein and patterns of HIV p24 immunohistochemistry in different brain areas of AIDS patients. *Aids* 2001, 15:571–575
39. Wong LH, Sim H, Chatterjee-Kishore M, Hatzinisiriou I, Devenish RJ, Stark G, Ralph SJ: Isolation and characterization of a human STAT1 gene regulatory element. Inducibility by interferon (IFN) types I and II and role of IFN regulatory factor-1. *J Biol Chem* 2002, 277:19408–19417
40. Labrada L, Liang XH, Zheng W, Johnston C, Levine B: Age-dependent resistance to lethal alphavirus encephalitis in mice: analysis of gene expression in the central nervous system and identification of a novel interferon-inducible protective gene, mouse ISG12. *J Virol* 2002, 76:11688–11703
41. Bigger CB, Brasky KM, Lanford RE: DNA microarray analysis of chimpanzee liver during acute resolving hepatitis C virus infection. *J Virol* 2001, 75:7059–7066
42. Zhu H, Cong JP, Mamtora G, Gingeras T, Shenk T: Cellular gene expression altered by human cytomegalovirus: global monitoring with



- oligonucleotide arrays. *Proc Natl Acad Sci USA* 1998, 95:14470–14475
43. Geimonen E, Neff S, Raymond T, Kocer SS, Gavrilovskaya IN, Mackow ER: Pathogenic and nonpathogenic hantaviruses differentially regulate endothelial cell responses. *Proc Natl Acad Sci USA* 2002, 99:13837–13842
  44. Piacentini M: Tissue transglutaminase: a candidate effector element of physiological cell death. *Curr Top Microbiol Immunol* 1995, 200:163–175
  45. Bergamini A, Capozzi M, Piacentini M: Macrophage-colony stimulating factor (M-CSF) stimulation induces cell death in HIV-infected human monocytes. *Immunol Lett* 1994, 42:35–40
  46. Nishiyama A, Matsui M, Iwata S, Hirota K, Masutani H, Nakamura H, Takagi Y, Sono H, Gon Y, Yodoi J: Identification of thioredoxin-binding protein-2/vitamin D(3) up-regulated protein 1 as a negative regulator of thioredoxin function and expression. *J Biol Chem* 1999, 274:21645–21650
  47. Junn E, Han SH, Im JY, Yang Y, Cho EW, Um HD, Kim DK, Lee KW, Han PL, Rhee SG, Choi I: Vitamin D3 up-regulated protein 1 mediates oxidative stress via suppressing the thioredoxin function. *J Immunol* 2000, 164:6287–6295
  48. Heyes MP, Ellis RJ, Ryan L, Childers ME, Grant I, Wolfson T, Archibald S, Jernigan TL: Elevated cerebrospinal fluid quinolinic acid levels are associated with region-specific cerebral volume loss in HIV infection. *Brain* 2001, 124:1033–1042
  49. Burudi EM, Marcondes MC, Watry DD, Zandonatti M, Taffe MA, Fox HS: Regulation of indoleamine 2, 3-dioxygenase expression in simian immunodeficiency virus-infected monkey brains. *J Virol* 2002, 76:12233–12241
  50. Siao CJ, Tsirka SE: Tissue plasminogen activator mediates microglial activation via its finger domain through annexin II. *J Neurosci* 2002, 22:3352–3358
  51. Jee Y, Kim G, Tanuma N, Matsumoto Y: STAT expression and localization in the central nervous system during autoimmune encephalomyelitis in Lewis rats. *J Neuroimmunol* 2001, 114:40–47
  52. Kim IJ, Beck HN, Lein PJ, Higgins D: Interferon gamma induces retrograde dendritic retraction and inhibits synapse formation. *J Neurosci* 2002, 22:4530–4539
  53. Piacentini M, Farrace MG, Piredda L, Matarrese P, Ciccocanti F, Falasca L, Rodolfo C, Giammarioli AM, Verderio E, Griffin M, Malorni W: Transglutaminase overexpression sensitizes neuronal cell lines to apoptosis by increasing mitochondrial membrane potential and cellular oxidative stress. *J Neurochem* 2002, 81:1061–1072
  54. Karpuj MV, Becher MW, Steinman L: Evidence for a role for transglutaminase in Huntington's disease and the potential therapeutic implications. *Neurochem Int* 2002, 40:31–36
  55. Dedeoglu A, Kubilus JK, Jeitner TM, Matson SA, Bogdanov M, Kowall NW, Matson WR, Cooper AJ, Ratan RR, Beal MF, Hersch SM, Ferrante RJ: Therapeutic effects of cystamine in a murine model of Huntington's disease. *J Neurosci* 2002, 22:8942–8950
  56. Lin X, Antalffy B, Kang D, Orr HT, Zoghbi HY: Polyglutamine expansion down-regulates specific neuronal genes before pathologic changes in SCA1. *Nat Neurosci* 2000, 3:157–163
  57. Fisher RP: CDKs and cyclins in transition(s). *Curr Opin Genet Dev* 1997, 7:32–38
  58. Farnham PJ, Slansky JE, Kollmar R: The role of E2F in the mammalian cell cycle. *Biochim Biophys Acta* 1993, 1155:125–131
  59. Adams PD, Kaelin Jr WG: The cellular effects of E2F overexpression. *Curr Top Microbiol Immunol* 1996, 208:79–93
  60. Giovanni A, Wirtz-Brugger F, Keramaris E, Slack R, Park DS: Involvement of cell cycle elements, cyclin-dependent kinases, pRb, and E2F x DP, in B-amyloid-induced neuronal death. *J Biol Chem* 1999, 274:19011–19016
  61. Jordan-Sciutto KL, Wang G, Murphy-Corb M, Wiley CA: Induction of cell-cycle regulators in simian immunodeficiency virus encephalitis. *Am J Pathol* 2000, 157:497–507
  62. Jordan-Sciutto KL, Wang G, Murphy-Corb M, Wiley CA: Cell cycle proteins exhibit altered expression patterns in lentiviral-associated encephalitis. *J Neurosci* 2002, 22:2185–2195
  63. Mendelsohn AR, Hamer JD, Wang ZB, Brent R: Cyclin D3 activates caspase 2, connecting cell proliferation with cell death. *Proc Natl Acad Sci USA* 2002, 99:6871–6876
  64. Garden GA, Budd SL, Tsai E, Hanson L, Kaul M, D'Emilia DM, Friedlander RM, Yuan J, Masliah E, Lipton SA: Caspase cascades in human immunodeficiency virus-associated neurodegeneration. *J Neurosci* 2002, 22:4015–4024